Biomedicine & Pharmacotherapy 87 (2017) 366–374

Available online at
ScienceDirect
www.sciencedirect.com

Elsevier Masson France
EM|consulte
www.em-consulte.com/en

Original article

# Loss of periplakin expression is associated with the tumorigenesis of colorectal carcinoma

Xiang Li[a,1], Guohui Zhang[a,1], Yan Wang[a], Ahmed Elgehama[a], Yang Sun[a], Lele Li[b], Yanhong Gu[b,1,**], Wenjie Guo[a,1,***], Qiang Xu[a,1,*]

[a] State Key Laboratory of Pharmaceutical Biotechnology, School of Life Science, Nanjing University, 163 Xianlin Avenue, Nanjing 210023, China
[b] Department of Oncology, The First Affiliated Hospital of Nanjing Medical University, Nanjing 210029, China

ARTICLE INFO

*Article history:*
Received 29 August 2016
Received in revised form 19 December 2016
Accepted 21 December 2016

*Keywords:*
Periplakin (PPL)
Tumorigenesis
Colorectal carcinoma
Cell cycle
Tumor suppressor

ABSTRACT

Periplakin (PPL), a member of the plakin protein family, has been reported to be down-expressed in urothelial carcinoma. The role of PPL in human colorectal cancer, however, remains largely unknown. Also little is known about the contribution of PPL to the malignant property of colorectal cancer and the intracellular function of PPL. In this study, we demonstrated that PPL was apparently down-expressed in colon carcinomas compared with normal and para-carcinoma tissues, which was correlated with the tumor size. Enforced expression of PPL in HT29 cells inhibited its proliferation evidenced by decreased expression of phosphorylated ERK and PCNA. Furthermore, PPL overexpression could reduce metastasis and epithelial-mesenchymal transition (EMT) of HT29 cells, with decreased expression of N-cadherin, Snail, Slug and α-SMA while increased expression of E-cadherin. On the contrary, the PPL knockdown could promote the cell proliferation, migratory, invasive and EMT ability of HT29 cells. Moreover, enforced expression of PPL induced G1/G0 cell cycle arrest, with decreased cyclin D1, p-Rb and increased expression of $p27^{kib}$, which could be reversed by PPL knockdown. In addition, PPL overexpression inhibited the growth of colon cancer allograft in vivo. Taken together, acted as a tumor suppressor in colon cancer progression, PPL could be a new biomarker or potential therapeutic target in colon cancer.


## 1. Introduction

Colorectal cancer is the first among the most three commonly diagnosed cancers worldwide, with more than 1.2 million new cases and half a million cases died every year [1,2]. Although much work has been done, the treatment of colon cancer is still dissatisfactory. Surgery alone always leads to tumor metastasis because of recurrence. And 5-Fluorouracil (5-FU) was the first chemotherapeutic agent widely used to treat colorectal cancer. However, high frequency of drug resistance limits its clinical efficacy [3]. Consequently, there is still an urgent need to seek for new targets and agents for colorectal cancer therapy.

Periplakin (PPL) is a 195 kDa membrane-associated protein and a member of the plakin protein family [4], which is mainly localized in the desmosomes and interdesmosomal plasma membranes of differentiated epidermal keratinocytes [5]. PPL is expressed in keratinized and nonkeratinized epithelial cells of the epidermis, the urinary bladder, the oral, the esophageal, and the colorectal [4]. It is reported that PPL is one of the candidates for a tumor marker for urothelial carcinoma [6].

On the other hand, PPL was reported to be significantly down-regulated in cancer tissues and scarcely expressed in advanced-stage of human esophageal cancers [7]. Also, the loss of PPL expression was associated with pathological stage and cancer-specific survival in patients with urothelial bladder cancer [8]. Moreover, the molecular mechanism underlying the regulation of PPL expression in the esophageal squamous cell carcinoma might be related to the aberrant DNA hypermethylation [9].

However, it was reported that plakin families function "molecular bridges" of cells that link the intracellular cytoskeleton and cell-cell junctions. PPL as an adhesion molecule plays a role in cellular movement and attachment in pharyngeal squamous cancer cell [10]. Although, PPL down-regulation is associated with

* Corresponding author at: School of Life Sciences, State Key Laboratory of Pharmaceutical Biotechnology, Nanjing University, Nanjing, 210023, China.
** Corresponding author at: Department of Clinical Oncology, The First Affiliated Hospital of Nanjing Medical University, Nanjing, 210029, China.
*** Corresponding author at: State Key Laboratory of Pharmaceutical Biotechnology, School of Life Sciences, Nanjing University, Nanjing, 210023, China.
*E-mail addresses:* guluer@163.com (Y. Gu), guowj@nju.edu.cn (W. Guo), molpharm@163.com (Q. Xu).
[1] These authors share co-first authorship.

http://dx.doi.org/10.1016/j.biopha.2016.12.103
0753-3322/

cancer progression. Its role in colorectal tumorigenesis has not been studied yet. The intracellular function of PPL is also not clear.

In this study, we assessed PPL expression in normal human colon tissue (N), para-carcinoma tissue (P) and tumor tissue (T). We have determined the potential clinical correlations to assess the loss of PPL if it could be a useful clinical phenomenon during cancer formation. We also investigated the antitumor effects and mechanism of PPL to determine its potential to be a candidate for colorectal carcinoma therapy.

## 2. Materials and methods

### 2.1. Reagents

3-(4, 5-dimethyl-2-thiazyl)-2, 5-diphenyl-2H-tetrazolium bromide (MTT) and puromycin were purchased from Sigma-Aldrich (St Louis, MO). TRIzol reagent and Lipofectamine® 3000 transfection reagent and cell culture products were obtained from Life technologies (Carlsbad, CA, USA). Propidium iodide (PI) was purchased from BD Biosciences (San Jose, CA). Streptavidin-HRP and DAB substrate were obtained from Genetech Company (Shanghai, China). Antibodies against phospho-Rb (Ser 807/811), Rb, cyclin D1, p21, $p27^{kip}$, N-cadherin, phospho-ERK1/2, ERK1/2 and Flag were purchased from Cell Signal Technology (Beverly, MA). Antibodies against α-SMA, PPL, PCNA, Slug, Snail and Actin were obtained from Santa Cruz Biotechnology (Santa Cruz, CA). PPL plasmid was obtained by Nanjing Jinuomei Biotech Company (Nanjing, China). Lentivirus vector and shRNA-PPL were obtained from ABM Biotechnology Company (Nanjing, China).

### 2.2. Human colorectal cancer samples

The primary colorectal cancer tissues (T) and their matching, adjacent normal colon tissue (N) tissues and para-carcinoma tissue (P) were collected from 50 colorectal cancer patients undergoing surgery at the First Affiliated Hospital of Nanjing Medical University, Nanjing, China. Informed consent was given in all patients examined. All samples were confirmed by pathological examination. Histological grade was defined according to the World Health Organization classification.

### 2.3. Reverse transcription-polymerase chain reaction and Real-time PCR

Total RNA from tissue samples was isolated using TRIzol reagent (Invitrogen, Carlsbad, CA, USA), according to the supplier's instructions. Approximately 1 μg total RNA was reverse transcribed into cDNA using Superscript II enzyme and oligo (dT) (Invitrogen). Real-time PCR was performed as follows: the cDNA was subjected to quantitative PCR, which was performed with the BioRad Real-Time PCR Detection System (Bio-Rad, CFX Connect TM SYBR® Green Supermix) (Bio-Rad, 1708880), and threshold cycle numbers were obtained using BioRad CFX Manager Software. The program for amplification was 1 cycle of 95 °C for 2 min followed by 40 cycles of 95 °C for 10 s, 60 °C for 30 s, and 95 °C for 10 s glyceraldehyde-3- phosphate dehydrogenase (GAPDH) was used as an internal control. The primer sequences used in this study are listed below, Primer: GAPDH, forward 5′-CGCATCTTCTTTTGCGTCGCC-3′, reverse 5′-TCCACGACGTACTCAGCGCCA −3′. PPL, forward 5′-AGTGACCTCCTTGGTGTCGT-3′, reverse 5′-AGG GTGAATGATGGTTGGG-3′. Snail, forward 5′-TCGGAAGCCTAACTACAGCGA −3′, reverse 5′-AGATGAGCATTGGCAGCGAG −3′. Slug, forward 5′-TCTCTGATCCCTCAATTTGGTCT −3′, reverse 5′-CCACACACAGGGTTAAAGTGTC−3′. Twist, forward 5′- GTCCGCAGTCTTACGAGGAG −3′, reverse 5′- GCTTGAGGGTCTGAATCTTGCT −3′.

### 2.4. Immunohistochemistry

Formalin-fixed paraffin-embedded tissue sections were deparaffinized in xylene, rehydrated through graded ethanol and then boiled for 10 min in citrate buffer (10 mM, pH 6.0) for antigen retrieval. Endogenous peroxidase activity was suppressed by exposure to 3% hydrogen peroxide for 10 min. Slides were then blocked with 3% goat serum (Life Technology, 16210-064), incubated with diluted PPL primary antibodies for 2 h at room temperature at 37 °C and then incubated with streptavidin-HRP (Shanghai Gene Company, GK500705) for 40 min, then stained with DAB (Shanghai Gene Company, GK500705) substrate and counter-stained with hematoxylin. Images were acquired by microscopy (Olympus FV1000). The immunohistochemical staining intensity was scored by immunoreactive score (IRS) and integral optical density (IOD).

### 2.5. Cell culture and cell proliferation assay

The human colon cancer cell HT29 and mouse colon cancer cell CT26 were purchased from the Shanghai Institute of Cell Biology (Shanghai, China). Cells were maintained in RPMI 1640 medium and DMEM medium (Gibco, USA) supplemented with 10% (v/v) fetal bovine serum (FBS) (Gibco, USA), antibiotics (100 U/ml penicillin and 100 μg/ml streptomycin), at 37 °C in a humidified atmosphere of 5% $CO^2$. Cell proliferation was determined by MTT assay as previously reported [11].

### 2.6. Plasmid transfection

Transient transfection of HT29 cells was performed using the Lipofectamine® 3000 (Invitrogen, Carlsbad, CA, USA) reagents by following the manufacturer's instructions. For stable expression, CT26 colon cancer cells were transfected with 4 μg of PPL plasmid (The backbone vector of this plasmid is pcDNA3.1), and the expression of PPL was confirmed by western blotting. At 48 h post transfection, the cells were selected with 600 mg/ml of Kanamycin, and the positive clones were picked up for further expansion.

### 2.7. Lentivirus infection

The lentivirus harboring human or mouse shRNA-PPL and vector (pLV-IRES-Puro) were purchased from ABM Biotech Company. The cells were infected with lentivirus with the MOI 5:1. The stable cell line was selected with 10 μg/ml of puromycin, and the positive clones were picked up for further expansion.

### 2.8. Transwell migration assay

Cells ($1 \times 10^5$/well) were plated into the top chamber and 10% FBS-containing medium was placed into the bottom chamber. After incubation at 37 °C in 5% $CO^2$ for 24 h, the cells remaining on the upper surface of the membrane were removed with a cotton swab. The cells that migrated through the 8-mm sized pores and adhered to the lower surface of the membrane were fixed with 4% paraformaldehyde, stained with 0.1% crystal violet and photographed by microscopy. The number of migration cells was assessed in 10 randomly selected fields under a microscope.

### 2.9. Colony-formation assay

Cells were harvested and seeded into the six-well plate (1000 cells/well) and incubated at 37 °C in a 5% $CO^2$ humidified incubator for 10 days. The medium was changed at 3-days interval. At the end of the incubation period, the cultures were fixed with 4% paraformaldehyde, stained with crystal violet and photographed.

Five visual fields of each group were selected in crystal violet staining, the colonies numbers have been counted under the microscopy and averaged.

### 2.10. Wound-healing assay

Cells were transfected with pcDNA3.1 and PPL plasmid. Then, cells were grown to confluence in 6-well plates, and monolayer cells were scraped using a micropipette (yellow) tip. After washing with PBS, serum-free medium was added to prevent cell proliferation. Photographs of the wounded area were taken immediately after the scratch was made. 12, 24, 48 and 72 h after scraping, cell movement into the wounded area was monitored by microscopy.

### 2.11. Transwell invasion assay

For the transwell invasion assay, the Mock and PPL overexpression HT29 cells, with 200 μl serum-free media were added to the upper compartment which was coated with 30 μl Matrigel (1:2 dilution; Costar, Corning, NY, USA). DMEM containing 10% FBS was added to the lower compartment, and further incubation was carried out for 24 h. The cells that penetrated the membrane of the chamber were stained with hematoxylin. The cells on the upper membrane were removed with a cotton tip. The number of invasive cells was assessed in 10 randomly selected fields under a microscope. The experiments were tested in triplicate.

### 2.12. Western blot

Cells were collected and centrifuged at 1,000*g*, washed with PBS, then the pellet was lysed in 100 μl precooling lysis buffer containing 0.5% Triton X-100, 100 mM Tris–HCl, 150 mM NaCl, 0.1 U/mL aprotinin and 1 mM phenylmethylsulfonyl fluoride for 30 min on ice and centrifuged at 12,000 g for 10 min. The supernatant was collected and followed by determination of protein concentration using the BCA protein assay kit (Pierce, 23225). Mixed with a double volume of sample buffer (62.5 mM Tris, pH 6.8, 2% SDS, 5% mercaptoethanol, 1% bromophenol blue, and 25% glycerol) and boiled for 5 min, 20 μg protein was separated on a 10% SDS-PAGE. Proteins were transferred to a polyvinylidene-difluoride (PVDF) membrane (Millipore, Bedford, MA), blocked by 5% nonfat milk for 1 h at room temperature, incubated overnight at 4 °C with indicated primary antibody, and then with a horseradish peroxidase-conjugated secondary antibody. Protein bands were visualized using Western blotting detection system according to the manufacturer's instructions (Cell Signaling Technology, MA).

### 2.13. Cell cycle assay

Cells were collected and washed with cold PBS and fixed with 70% ethanol at 4 °C overnight. Then, the fixed cells were washed with PBS and stained with 50 μg/ml of PI-containing 100 μg/ml of RNase A and 1% Triton X-100 in the dark at room temperature for 30 min. The DNA contents of the cells were detected by FACS and analyzed with Modfit software (Becton Dickinson, San Jose, CA).

### 2.14. Animal model

Twenty male BALB/c mice, 4–6 weeks old, were purchased from the Model Animal Research Center of Nanjing University (Nanjing, China). They were maintained with free access to pellet food and water in plastic cages at 21 ± 2 °C and kept on a 12 h light/dark cycle. Animal welfare and experimental procedures were performed in accordance with the Guide for the Care and Use of Laboratory Animals (National Institutes of Health, the United States) and the related ethical regulations of our university. All efforts were made to reduce the number of animals used and to minimize animals' suffering. These mice were randomly divided into two groups (ten mice/group). Both groups received subcutaneous injections of either vector or PPL-overexpressing CT26 cells ($2 \times 10^6$ cells in 100 μl PBS) on the right side of axillary of each mouse. Tumor growth was evaluated by measuring the length and width of the tumor mass with calipers every 2 days. Tumor volumes were calculated by the modified ellipsoidal formula: $(\text{length} \times \text{width}^2)/2$.

### 2.15. Statistical analysis

All results shown represent means ± SEM from triplicate experiments performed in a parallel manner. Data were statistically evaluated by one-way ANOVA followed by Dunnett's test between the control group and multiple dose groups. The level of significance was set at a *P*-value of 0.05.

## 3. Results

### 3.1. PPL is down-regulated in colorectal cancer

To assess the expression of PPL in colorectal cancer, PPL mRNA was evaluated by real-time PCR in 50 paired normal colon tissues and colorectal cancer tissues. The results showed that PPL mRNA levels were down-regulated in colorectal cancer tissues compared to normal colon tissues (Fig. 1A). Next, we determined the PPL protein level by immunohistochemical staining and found that PPL protein levels were also down expressed with the tumorigenesis of colorectal carcinoma (Fig. 1B), showing by the arrow. Then the histology score of colorectal cancer tissues (T) and their matching, adjacent normal colon tissues (N) and para-carcinoma tissues (P) was evaluated, which was significantly decreased in para-carcinoma tissues and cancer tissues (Fig. 1C). Moreover, the expression of PPL was associated with the tumor volume, the lower expression the bigger volume (Fig. 1E). However, no significant differences were observed between PPL level and Dukes' stage, which may be due to the number of the samples (Fig. 1D).

### 3.2. PPL overexpression reduces the proliferation of HT29 cells

Based on the loss of PPL in colon cancer tissues compared to normal tissues, the tumor suppressor properties of PPL were investigated by MTT and colony formation assays. We transiently transfected PPL-expressed plasmid to HT29 cells and the expression of PPL in HT29 cells was confirmed by real-time PCR and western blot (Fig. 2A). The PPL-overexpressing HT29 cells slowly grew and detected by MTT assay and the morphology (Figure B), and formed fewer clones than the mock cells (Fig. 2C). To better understand the effects of PPL overexpression on HT29 cell growth, we analyzed the expression of various proteins related to cell proliferation by using western blot. The results showed that PPL overexpression reduced the levels of phosphorylated ERK1/2 and proliferating cell nuclear antigen (PCNA) (Fig. 2D).

### 3.3. PPL overexpression reduces the migratory, invasive and EMT ability of HT29 cells

In addition, the wound closure of the PPL-transfected HT29 cells was remarkably delayed compared with that of the mock-transfected cells in the wound-healing assay for 0, 24, 48 and 72 h (Fig. 3A). The relative field was significantly decreased in the PPL overexpression group, with 25% and 50% in 48 and 72 h, respectively. Furthermore, we determined the role of PPL in HT29

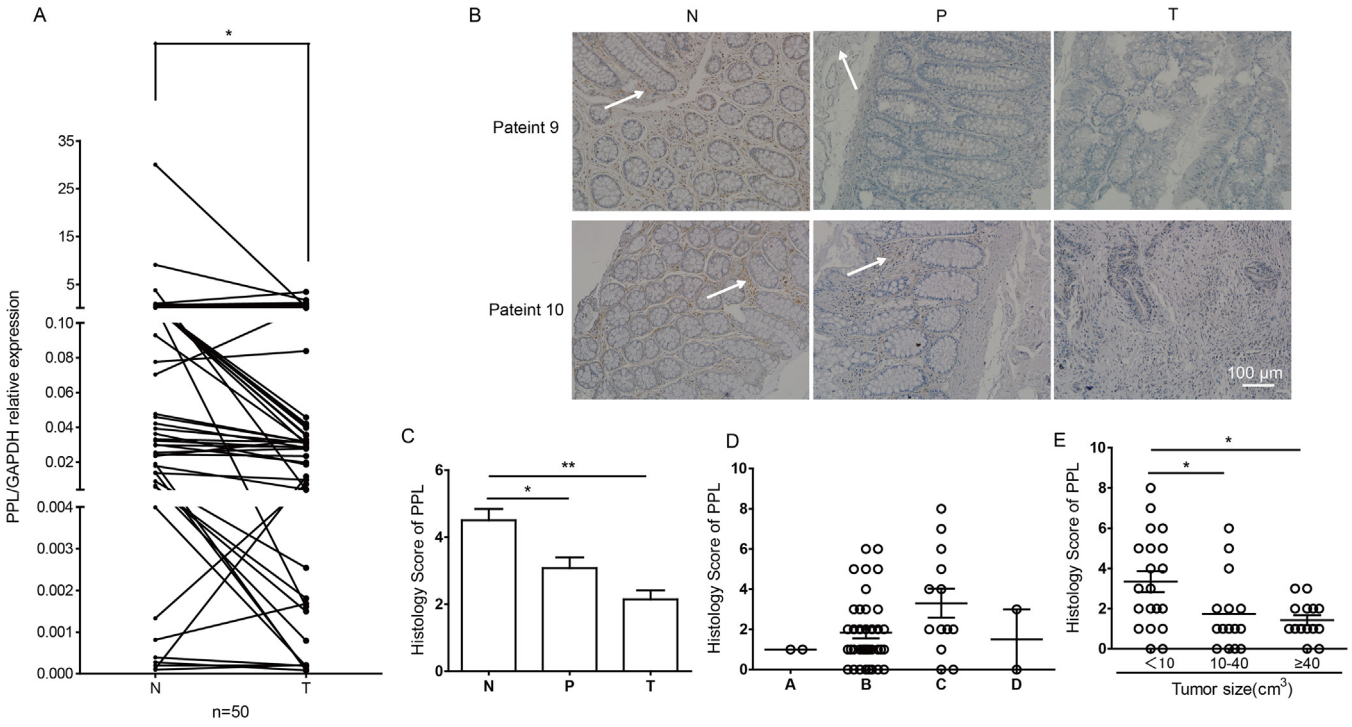


**Fig. 1.** Periplakin (PPL) expression in colorectal cancer tissues and paired adjacent normal tissues.
(A) Real-time RT-PCR analyses of PPL mRNA levels in colorectal cancer (T) and normal colorectal (N) tissues. Solid line indicates matched samples. (B) Immunohistochemical staining of PPL in representative colorectal cancer tissues (T), their matching adjacent normal colon tissues (N) and para-carcinoma tissues (P). Original magnification 200×. (C) The histology score of PPL on T, N and P of 50 patients. (D) Correlation between Dukes'stage and PPL histology score. (E) Correlation between tumor sizes and PPL histology score. The data above were presented as means ± SEM. One-way ANOVA revealed a significant difference at $^{*}P < 0.05$, $^{**}P < 0.01$ versus normal group (n = 50).

colon cancer cell motility by using transwell migration assay. Compared with the mock cells, PPL overexpression markedly reduced the number of migrated HT29 cells (Fig. 3B). Also, PPL overexpression could obviously reduce the number of invasion HT29 cells (Fig. 3C). The role of PPL in cell migration led us to examine if it had any effect on EMT in colon cancer cells. The

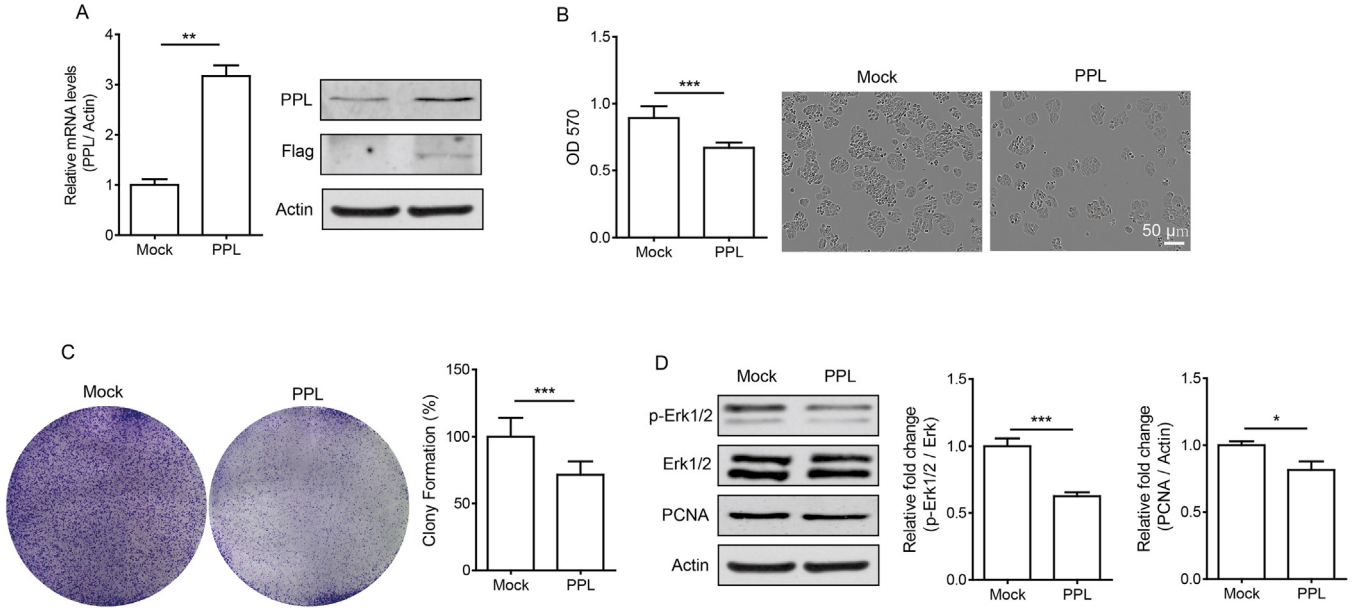


**Fig. 2.** PPL overexpression reduces the proliferation of HT29 cells.
(A) Real-time RT-PCR and western blot analyses of PPL expression in transfected HT29 cells, $^{**}P < 0.01$. (B) The growth of mock and PPL-overexpressing HT29 cells was determined by MTT assay. Each column represents the mean of the data from three independent experiments. The photographs were taken at a magnification 200×. (C) Representative images of colony formation in mock and PPL-overexpressing HT29 cells, and the colonies were quantified. Original magnification, 100×. (D) The expression of ERK, p-ERK and PCNA proteins in mock and PPL-overexpressing HT29 cells was examined by western blot and quantified by gray scale scanning used Image J. All the data were presented as means ± SEM of three independent experiments performed in triplicate. One-way ANOVA revealed a significant difference at $^{*}P < 0.05$, $^{**}P < 0.01$ and $^{***}P < 0.001$ versus mock group.

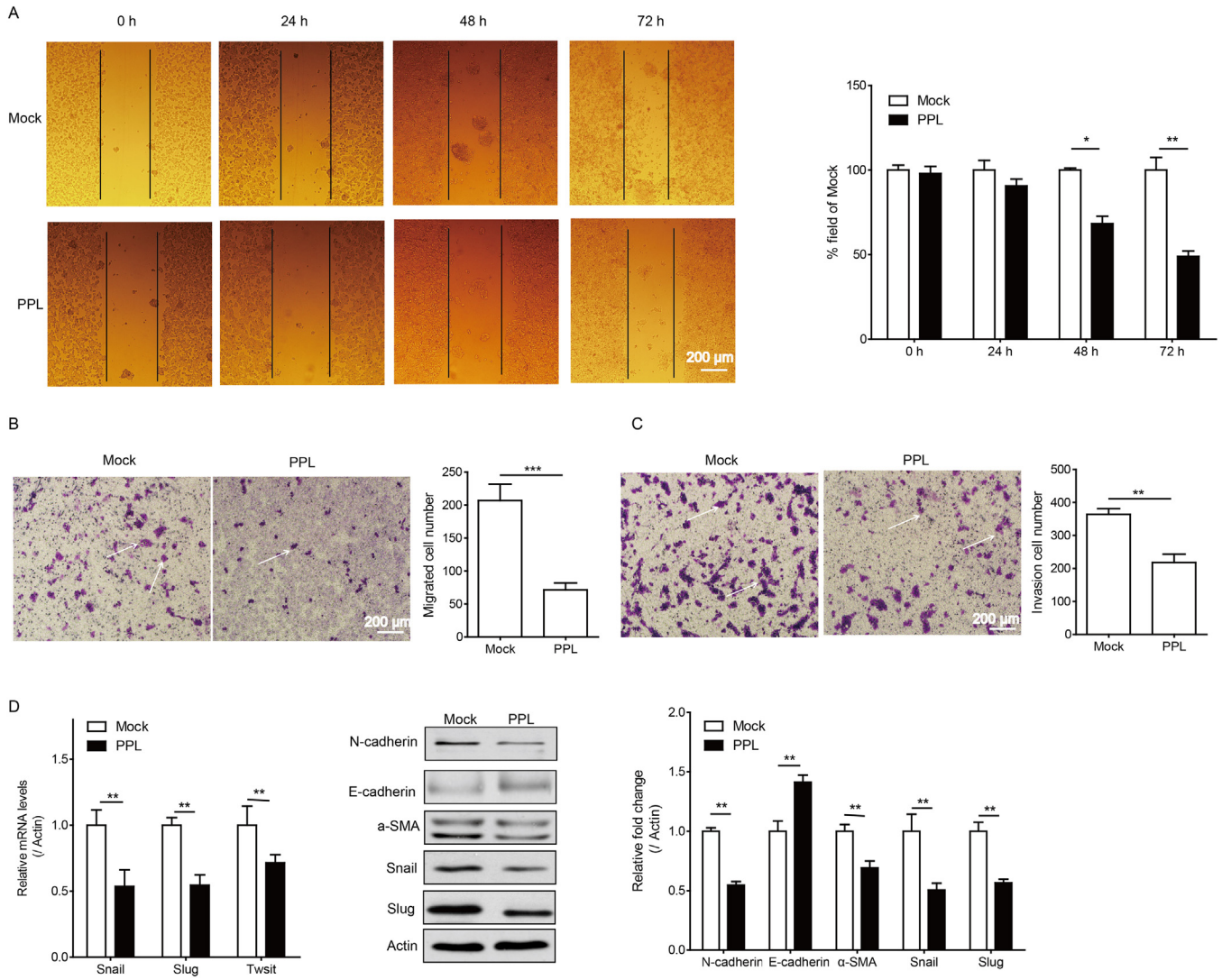


**Fig. 3.** PPL overexpression reduces the migratory and EMT ability of HT29 cells.
HT29 were tansfected with mock and PPL plasmid. (A) Representative images of wound healing of mock and PPL-overexpressing HT29 cells. The photographs were taken at a magnification 100×, and the wound closure was quantified. Cells were grown to confluence and then wounded by scraping. For each wound, the width of the wound at 0 h was designated as 100%, and the subsequent timepoints in the graph show the relative width of the open wound. Values represent the mean ± SEM from three independent experiments. (B) The migratory ability of mock and PPL-transfected HT29 cells was evaluated by transwell migration assay. And the number of migrated cells was quantified. Original magnification, 100×. (C) The invasive ability of mock and PPL-transfected HT29 cells was evaluated by transwell invasion assay. And the number of migrated and invaded cells was quantified. Original magnification, 100×. (D) The mRNA levels of Snail, Slug and Twsit were detected by QPCR. The expression of N-cadherin, E-cadherin, α-SMA, Snail and Slug proteins in mock and PPL-overexpressing HT29 cells was examined by western blot and quantified by gray scale scanning used Image J. All the data were presented as means ± SEM of three independent experiments performed in triplicate. One-way ANOVA revealed a significant difference at $^{*}P < 0.05$, $^{**}P < 0.01$ and $^{***}P < 0.001$ versus mock group.

expression of EMT-related proteins was detected by western blot and we found that PPL overexpression decreased the level of mesenchymal cell marker (N-cadherin,α-SMA, Snail, and Slug) and increased the level of epithelial cell marker (E-cadherin)(Fig. 3D). Thus, taken together, our results suggest that PPL overexpression inhibits the HT29 cell migration and EMT in vitro.

### *3.4. Loss of PPL elevate the proliferation, migratory and EMT ability of HT29 cells*

As HT29 has a basal level expression of PPL already, we used shRNA to knockdown PPL and tested whether cell proliferation or invasion was promoted. As expected, the PPL knockdown HT29 cells have grown faster, which were confirmed by real-time PCR and western blot (Fig. 4A). Also, the knockdown cells formed more clones than the control cells (Fig. 4B). Contrary to the PPL overexpression cells, the expression of phosphorylated ERK1/2 and PCNA in PPL knockdown cells were elevated (Fig. 4C).

Moreover, we detected the effect of PPL knockdown on the cell migration. The results showed that the wound closure of the PPL knockdown cells was faster than the control cells for 0, 24 and 48 h. The relative field was significantly increased in the PPL over-expression group, with 50% and 100% in 24 and 48 h respectively (Fig. 4D). Consistent with this, PPL knockdown also led to enhancement of the cell's EMT ability, showing that the transcription of Snail, Slug and Twist increased, the expression of N-cadherin, α-SMA, Snail and Slug up-regulated and the E-cadherin expression down-regulated.

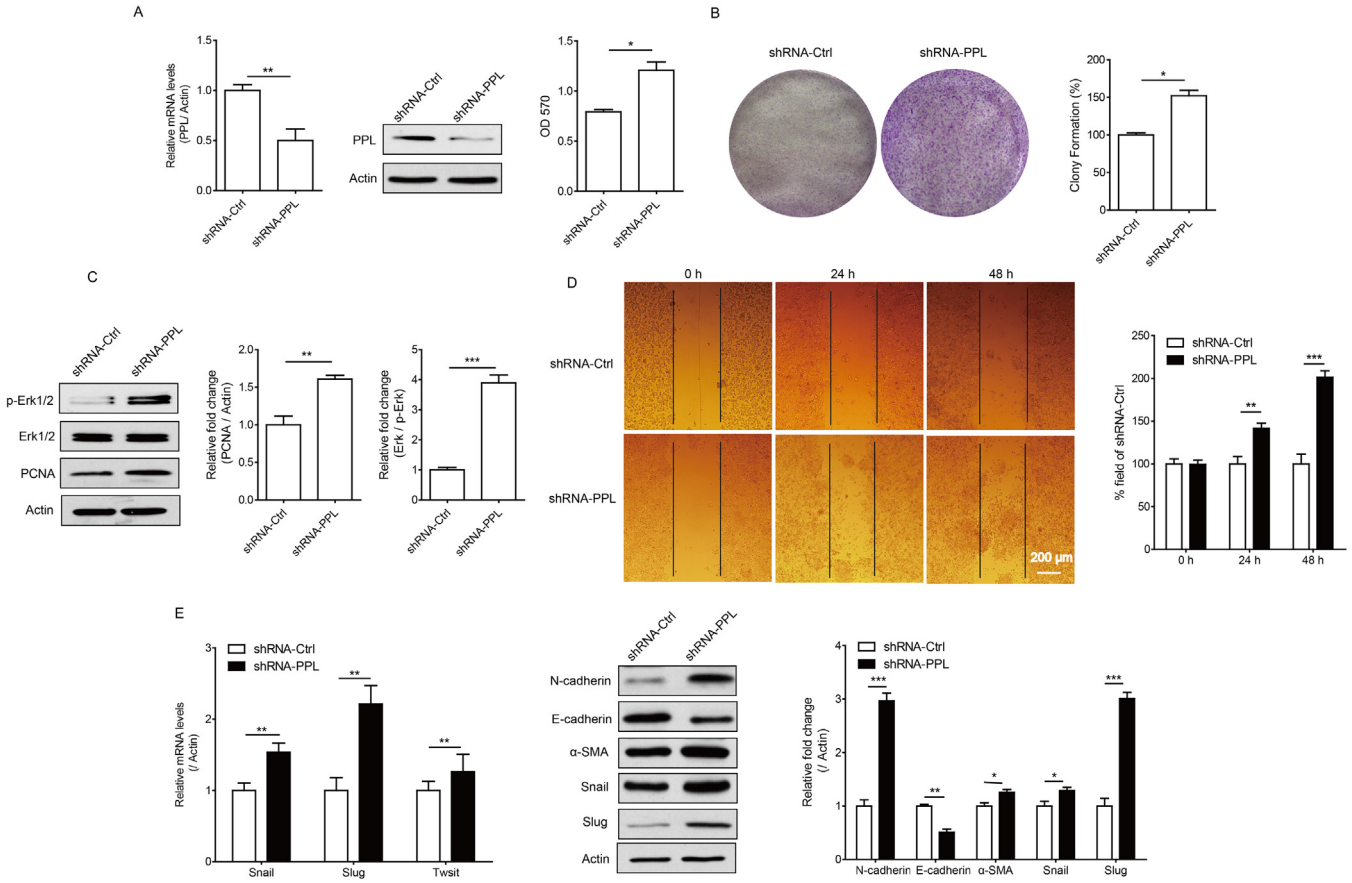


**Fig. 4.** Loss of PPL promote the proliferation, migratory and EMT ability of HT29 cells.
(A) Real-time RT-PCR and western blot analyses of PPL expression in infected HT29 cells, $^{**}P < 0.01$. The growth of shRNA-Ctrl and shRNA-PPL HT29 cells were determined by MTT assay. Each column represents the mean of the data from three independent experiments. (B) Representative images of colony formation in shRNA-Ctrl and shRNA-PPL HT29 cells, and the colonies were quantified. Original magnification, 100×. (C) The expression of ERK, p-ERK and PCNA proteins in shRNA-Ctrl and shRNA-PPL HT29 cells were examined by western blot and quantified by gray scale scanning used Image J. (D) Representative images of wound healing of shRNA-Ctrl and shRNA-PPL HT29 cells. The photographs were taken at a magnification 100×, and the wound closure was quantified. Cells were grown to confluence and then wounded by scraping. For each wound, the width of the wound at 0 h was designated as 100%, and the subsequent timepoints in the graph show the relative width of the open wound. Values represent the mean ± SEM from three independent experiments. (E) The mRNA levels of Snai, Slug and Twsit were detected by QPCR. The expression of N-cadherin, E-cadherin, α-SMA, Snail and Slug proteins in shRNA-Ctrl and shRNA-PPL HT29 cells was examined by western blot and quantified by gray scale scanning used Image J. All the data above were presented as means ± SEM of three independent experiments performed in triplicate. One-way ANOVA revealed a significant difference at $^{*}P < 0.05$, $^{**}P < 0.01$ and $^{***}P < 0.001$ versus shRNA-PPL group.

All above, the data suggest that loss of PPL could promote the proliferation of HT29 cells and elevate its migration and EMT ability.

### 3.5. PPL expression induces G0/G1 cell cycle arrest

To investigate the antiproliferative mechanism of PPL, cell cycle distributions of mock-transfected and PPL-transfected were analyzed by flow cytometry. Flow cytometric analysis showed that compared with mock cells, the PPL-overexpressing cell population had a higher rate in G1/G0 phase and a lower number of cells in S and G2/M phase (Fig. 5A and B). To obtain further insight into the mechanistic role of PPL in cell cycle arrest of HT29 cells, we examined the expression level of proteins which were involved in G1/G0 phase cycling including cyclin D1, CDK inhibitor p21, $p27^{kip}$ and p-Rb. Compared to the mock, PPL overexpression reduced the level of cyclin D1 and p-Rb, and elevated the level of $p27^{kip}$ (Fig. 5C). The expression of p21 was slightly elevated, but there is no significant difference. Moreover, we used shRNA to knockdown the PPL expression in the PPL-overexpression group for further confirmation on the effect of PPL on G0/G1 cell cycle arrest. We found that PPL knockdown could reverse partly the G0/G1 cell cycle arrest by PPL overexpression (Fig. 5D). Therefore, our data suggested that PPL is crucial for cell growth and cell cycle regulation in colorectal cancer cells.

### 3.6. Anti-tumor effects of PPL in animal studies

To investigate whether PPL overexpression could inhibit colon cancer growth in vivo, we generated the PPL-overexpressing CT26 cells to establish allograft tumor model in Balb/c mice. The stable expression of PPL in CT26 cells was confirmed by western blot and immunohistochemistry (Fig. 6A and F). PPL-overexpressing CT26 cells formed subcutaneous tumors fewer than mock cells. The tumors in PPL-overexpressing group grew slower, and the tumor weight was lower than that in the mock group (Fig. 6 B and C). Consistent with the clinical samples, the PPL protein levels (within Mock and PPL group) were negatively correlated with the tumor size (Fig. 6D). Compared with the mock group, the expression of PCNA and p-ERK were significantly decreased in allograft tumors in PPL-overexpressing group which is consistent with our results in vitro. Also as expected, the E-cadherin expression was increased,

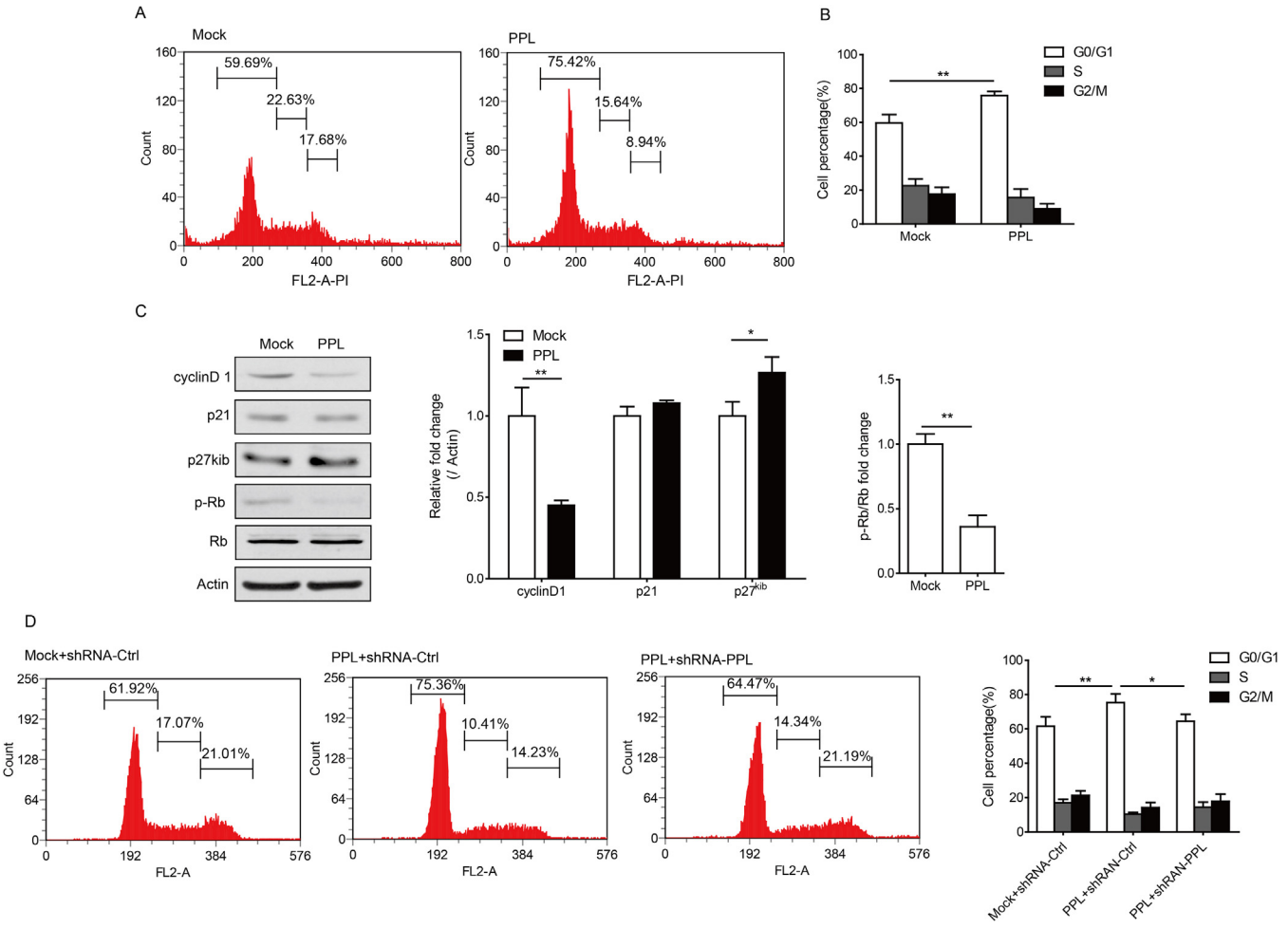


**Fig. 5.** PPL overexpression caused cell cycle arrest in G0/G1 phase in HT29 cells.
HT29 were tansfected with mock and PPL plasmid. (A) HT29 cells were stained by PI and analyzed by flow cytometry. (B) The data represented here is average of three independent experiments. (C) Mock and PPL overexpressed HT29 cells were harvested and lysed, and then the expression of cell cycle-related proteins was analyzed by western blot. The quantification of each protein was gray scale scanned by Image J. The quantity data was presented as means ± SEM of three independent experiments performed in triplicate. One-way ANOVA revealed a significant difference at $^{*}P < 0.05$, $^{**}P < 0.01$ and $^{***}P < 0.001$ versus mock group. (D) PPL overexpressed HT29 cells were infected with shRNA-PPL, then the Mock, PPL overexpressed and PPL expressed + shRNA-PPL were harvested and stained by PI and analyzed by flow cytometry. The data represented here is average of three independent experiments with similar results.

whereas that of α-SMA and N-cadherin was decreased (Fig. 6E). The immunohistochemistry for PCNA also showed the same results that PPL overexpression decreased the expression of PCNA (Fig. 6F).

Furthermore, the PPL knockdown CT26 cells were constructed, which was confirmed by western blot. On the contrary, the PPL knockdown cells formed subcutaneous tumors faster and bigger than shRNA-Ctrl cells, and the tumor weight was higher. As expected, the expression of phosphorylated ERK1/2 and PCNA were elevated in PPL knockdown group (Fig. 6G).

## 4. Discussion

Selecting the beneficial treatment regimen for colorectal cancer remains challenging because of the lack of prognostic biomarkers [12]. Several studies have been done for the therapeutic target of colorectal carcinoma, but none have been proved to show satisfactory for colorectal carcinoma therapy [13,14]. Thus, to improve the diagnosis and prognosis of colorectal cancer, it is of great importance to get a full understanding of the molecular mechanisms underlying its carcinogenesis. In this study, we found that PPL, a urinary bladder marker [8], was down-regulated during the progression of the colon cancer (Fig. 1A–C). As expected, the PPL level was negatively associated with the tumor sizes in patients (Fig. 1E). We suppose that PPL may play important role in the colon cancer genesis. However, there was no significant difference between PPL level and the Dukes' stage, which would be limited by a relatively small sample size (Fig. 1D). Taken together, these results suggested that loss of PPL might be a useful biomarker for colon cancer progress.

For the loss of PPL in colon cancer tissues compared to normal tissues, we guess PPL may have tumor suppressor properties. To confirm our hypothesis, we demonstrated that PPL overexpression could inhibit the cancer cell proliferation (Fig. 2B&2C) and PPL knockdown could promote the cell proliferation (Fig. 4A & B) *in vitro* and *in vivo* (Fig. 6). To our knowledge, PCNA plays an important role in cell proliferation [15]. And numerous studies have reported that ERK1/2 acts as a mitogen-activated factor which is believed to mediate both cell proliferation and survival [16,17]. In this study, we found that PPL overexpression could reduce the expression of PCNA and p-ERK1/2 (Fig. 2D). Otherwise, PPL knockdown would up-regulate the PCNA and ERK1/2 expression (Fig. 4C). Thus, PPL could exert tumor suppressor properties.

Moreover, metastasis is one of the malignant properties of cancer and the major cause of cancer death [18]. Meanwhile, a report has shown that PPL is involved in cellular movement and attachment in pharyngeal squamous cancer cells [10]. Comparing

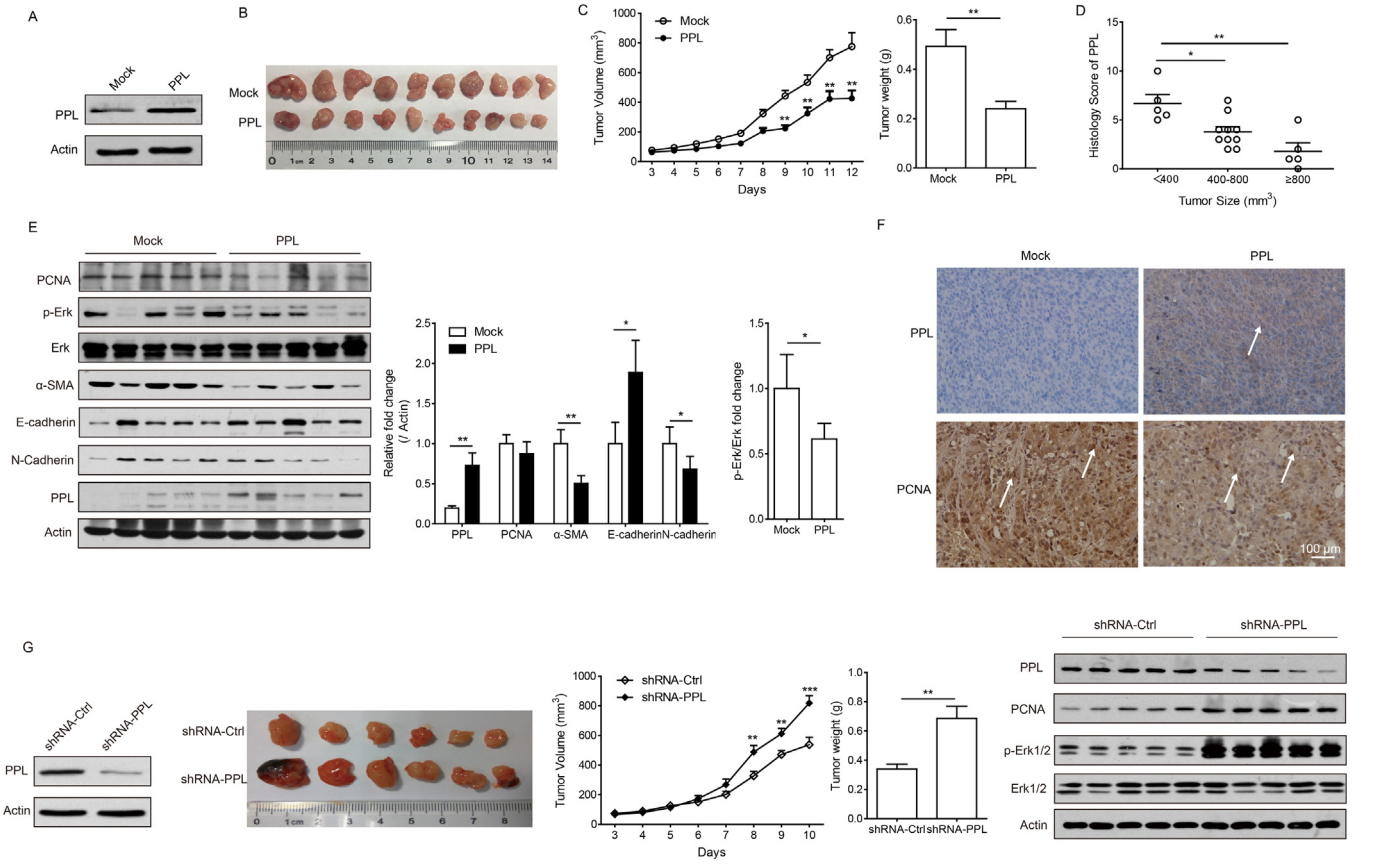


**Fig. 6.** PPL inhibits colorectal cancer progression in vivo.
CT26 cells were tansfected with mock and PPL plasmid. (A) Western blot analyses of PPL expression in stably transfected CT26 cells. (B) Images of tumor were evaluated in mice transplanted with mock and PPL-overexpressing CT26 cells. (C) Tumor growth curves and tumor weight was evaluated (n = 10). The data were presented as means ± SEM of three independent experiments performed. One-way ANOVA revealed a significant difference at $^{*}P < 0.05$, $^{**}P < 0.01$ and $^{***}P < 0.001$ versus mock group. (D) Correlation between tumor sizes and PPL (Both mock and PPL group) histology score. (E) The expressions of PPL, ERK, p-ERK, PCNA, N-cadherin, E-cadherin and α-SMA in allograft tumors were detected by western blot and quantified by gray scale scanning used Image J. (F) Representative images of PPL and PCNA immunohistochemical staining from mock and PPL overexpressed tumor tissue. Original magnification, 200×. (G) PPL was knockdown in CT26 cells by lentivirus infection. Western blot analyses of PPL expression in stably knockdown CT26 cells. Images of tumor were evaluated in mice transplanted with shRNA-Ctrl and shRNA-PPL CT26 cells. Tumor growth curves and tumor weight was evaluated (n = 6). The data were presented as means ± SEM of three independent experiments performed. One-way ANOVA revealed a significant difference at $^{*}P < 0.05$, $^{**}P < 0.01$ and $^{***}P < 0.001$ versus shRNA-PPL group.

with this, our results showed that PPL high expression could reduce colon cancer cell migratory and invasive activity by wound closure and transwell migration assay (Fig. 3A-C). Moreover, EMT is an important process during cancer cell metastasis. In this study, compared with mock, PPL overexpression could reduce the level of mesenchymal markers (N-cadherin, α-SMA, Snail, and Slug), but increase the level of the epithelial marker (E-cadherin) (Fig. 3D). On the other hand, the knockdown of PPL in HT29 could elevate the cell migratory and EMT ability (Fig. 4D & E). As a result, loss of PPL may promote the EMT of colon cancer cells and result in tumor metastasis.

Additionally, our study showed that regulation of the cell cycle, particularly G0/G1 phase may be the intracellular function of PPL (Fig. 5A & B). Among the cell cycle related proteins, cyclin D1, a $G_1$-phase cell cycle molecule, can shorten the $G_1$-phase [19]. The phosphorylated Rb plays a core role in helping cells entry into the S phase, while the CDK inhibitor p21 and $p27^{kip}$ could inhibit cell growth by blocking the phase transition from $G_1$ to S [20,21]. Further exploring the underlying mechanisms of PPL on cell cycle arrest, we detected the effect of PPL on the expression of these proteins regulating phase transitions in cell cycle progression. After PPL overexpressing in HT29 cells, the level of p-Rb and cyclin D1 were decreased, whereas the expression of $p27^{kip}$ increased (Fig. 5C), indicating that PPL could be a cell cycle regulator. Also, the knockdown of PPL in the PPL overexpression group could partly reverse the G0/G1 phase arrest coursed by PPL (Fig. 5D). Therefore, cancer cells that with the loss of PPL might bypass the G1/G0 checkpoint, resulting in uncontrolled proliferation. In conclusion, this study showed that aberrant loss of PPL occurred in colorectal carcinomas progression and was significantly associated with tumor malignancy. Furthermore, PPL acted as a tumor suppressor by inhibiting cancer cell proliferation and tumor growth, reducing the activity of migratory and EMT, and inducing G1/G0 cell cycle arrest of colon cancer cells. Therefore, PPL could be a potential therapeutic in colon cancer.

## Conflict of interest

The authors state no conflict of interest.

## Acknowledgments

This work was supported by the National Natural Science Foundation of China (91429308, 81572389), Jiangsu Province Clinical Science and Technology Project (Clinical Research Center, BL2012008), and Key Personnel of Jiangsu Province (RC2011170).

## References


[1] A. Jemal, F. Bray, M.M. Center, J. Ferlay, E. Ward, D. Forman, Global cancer statistics, CA Cancer J. Clin. 61 (2011) 69–90.

[2] J. Ferlay, H.R. Shin, F. Bray, D. Forman, C. Mathers, D.M. Parkin, Estimates of worldwide burden of cancer in 2008: GLOBOCAN 2008, Int. J. Cancer 127 (2010) 2893–2917.

[3] B. Iovine, F. Guardia, C. Irace, M.A. Bevilacqua, l-carnosine dipeptide overcomes acquired resistance to 5-fluorouracil in HT29 human colon cancer cells via downregulation of HIF1-alpha and induction of apoptosis, Biochimie (2016), doi:http://dx.doi.org/10.1016/j.biochi.2016.05.010.

[4] C. Ruhrberg, M.A. Hajibagheri, D.A. Parry, F.M. Watt Periplakin, a novel component of cornified envelopes and desmosomes that belongs to the plakin family and forms complexes with envoplakin, J. Cell Biol. 139 (1997) 1835–1849.

[5] M. Simon, H. Green, Participation of membrane-associated proteins in the formation of the cross-linked envelope of the keratinocyte, Cell 36 (1984) 827–834.

[6] Y.K. Hiroshi Okusa, Masamichi Oh-Ishi, Yutaka Minamida1, N.K. Mayumi Tsuchida, Kazumasa Matsumoto, Takefumi Sato, T.M. Masatsugu Iwamura, Shiro Baba, Searching for new biomarkers of bladder cancer based on proteomic analysis, J. Electrophoresis 52 (2008) 19–24.

[7] T. Nishimori, T. Tomonaga, K. Matsushita, M. Oh-Ishi, Y. Kodera, T. Maeda, F. Nomura, H. Matsubara, H. Shimada, T. Ochiai, Proteomic analysis of primary esophageal squamous cell carcinoma reveals downregulation of a cell adhesion protein periplakin, Proteomics 6 (2006) 1011–1018.

[8] K. Matsumoto, M. Ikeda, Y. Sato, H. Kuruma, Y. Kamata, T. Nishimori, T. Tomonaga, F. Nomura, S. Egawa, M. Iwamura, Loss of periplakin expression is associated with pathological stage and cancer-specific survival in patients with urothelial carcinoma of the urinary bladder, Biomed. Res. 35 (2014) 201–206.

[9] T. Otsubo, T. Hagiwara, M. Tamura-Nakano, T. Sezaki, O. Miyake, C. Hinohara, T. Shimizu, K. Yamada, T. Dohi, Y.I. Kawamura, Aberrant DNA hypermethylation reduces the expression of the desmosome-related molecule periplakin in esophageal squamous cell carcinoma, Cancer Med. 4 (2015) 415–425.

[10] Y. Tonoike, K. Matsushita, T. Tomonaga, K. Katada, N. Tanaka, H. Shimada, Y. Nakatani, Y. Okamoto, F. Nomura, Adhesion molecule periplakin is involved in cellular movement and attachment in pharyngeal squamous cancer cells, BMC Cell Biol. 12 (2011) 41.

[11] X. Wang, X. Wu, A. Zhang, S. Wang, C. Hu, W. Chen, Y. Shen, R. Tan, Y. Sun, Q. Xu, Targeting the PDGF-B/PDGFR-β Interface with Destruxin A5 to Selectively Block PDGF-BB/PDGFR-ββ Signaling and Attenuate Liver Fibrosis, EBioMedicine 7 (2016) 146–156.

[12] H.S. Kim, S.J. Park, K.Y. Lee, Y.K. Park, Y.W. Kim, Reduced Raf-1 kinase inhibitor protein expression predicts less favorable outcomes in patients with hepatic colorectal metastasis, Oncol. Rep. 28 (2012) 161–171.

[13] H. Zheng, R. Ma, Q. Wang, P. Zhang, D. Li, Q. Wang, J. Wang, H. Li, H. Liu, Z. Wang, MiR-625-3p promotes cell migration and invasion via inhibition of SCAI in colorectal carcinoma cells, Oncotarget 6 (2015) 27805–27815.

[14] H.S. Kim, G. Yoon, S.I. Do, S.J. Kim, Y.W. Kim, Down-regulation of osteoprotegerin expression as a novel biomarker for colorectal carcinoma, Oncotarget 7 (2016) 15187–15199.

[15] M. Jurikova, L. Danihel, S. Polak, I. Varga, Ki67, PCNA, and MCM proteins: markers of proliferation in the diagnosis of breast cancer, Acta Histochem. 118 (2016) 544–552.

[16] J. Cao, R.C. Heijkants, A.G. Jochemsen, M. Dogrusoz, M.J. de Lange, P.A. van der Velden, S.H. van der Burg, M.J. Jager, R.M. Verdijk, Targeting of the MAPK and AKT pathways in conjunctival melanoma shows potential synergy, Oncotarget (2016), doi:http://dx.doi.org/10.18632/oncotarget.10770.

[17] G. Meng, K. Chai, X. Li, Y. Zhu, W. Huang, Luteolin exerts pro-apoptotic effect and anti-migration effects on A549 lung adenocarcinoma cells through the activation of MEK/ERK signaling pathway, Chem. Biol. Interact. 257 (2016) 26–34.

[18] K.S. Kopanska, Y. Alcheikh, R. Staneva, D. Vignjevic, T. Betz, Tensile forces originating from cancer spheroids facilitate tumor invasion, PLoS One 11 (2016) e0156442.

[19] R. Tapia, M. Huerta, S. Islas, A. Avila-Flores, E. Lopez-Bayghen, J. Weiske, O. Huber, L. Gonzalez-Mariscal, Zona occludens-2 inhibits cyclin D1 expression and cell proliferation and exhibits changes in localization along the cell cycle, Mol. Biol. Cell 20 (2009) 1102–1117.

[20] H. Shi, S. Chen, H. Jin, C. Xu, G. Dong, Q. Zhao, W. Wang, H. Zhang, W. Lin, J. Zhang, L. Davidovic, L. Yao, D. Fan, Downregulation of MSP58 inhibits growth of human colorectal cancer cells via regulation of the cyclin D1-cyclin-dependent kinase 4-p21 pathway, Cancer Sci. 100 (2009) 1585–1590.

[21] T. Onishi, K. Yamakawa, O.E. Franco, R. Suzuki, J. Kawamura, p27Kip1 is the key mediator of phenylacetate induced cell cycle arrest in human prostate cancer cells, Anticancer Res. 20 (2000) 3075–3081.